Neuron 49, 357–363, February 2, 2006 ©2006 Elsevier Inc. DOI 10.1016/j.neuron.2005.12.026

Strong Single-Fiber Sensory Inputs to Olfactory Cortex: Implications for Olfactory Coding

Report

Kevin M. Franks[1,2,*] and Jeffry S. Isaacson[1]
[1] Department of Neuroscience
University of California, San Diego
School of Medicine
La Jolla, California 92093

Summary

Olfactory information is first encoded in a combinatorial fashion by olfactory bulb glomeruli, which individually represent distinct chemical features of odors. This information is then transmitted to piriform (olfactory) cortex, via axons of olfactory bulb mitral and tufted (M/T) cells, where it is presumed to form the odor percept. However, mechanisms governing the integration of sensory information in mammalian olfactory cortex are unclear. Here we show that single M/T cells can make powerful connections with cortical pyramidal cells, and coincident input from few M/T cells is sufficient to elicit spike output. These findings suggest that odor coding is broad and distributed in olfactory cortex.

Introduction

At early stages of sensory processing, complex objects (such as images and sounds) are encoded as a combination of simpler components (edges and tones). A singular sensory percept is formed when these simple components are then decoded and combined in higher brain structures. In the mammalian olfactory system, odorant molecules are detected by olfactory receptor neurons (ORNs) in the nasal epithelium (Firestein, 2001). In rodents, signals from ~1000 different types of odorant receptors (ORs) map onto ~1800 glomeruli in the olfactory bulb, and sensory neurons expressing one unique OR project onto ~50 to 100 M/T cells within each glomerulus (Mombaerts et al., 1996). Because unique types of ORs are mapped to different glomeruli, each M/T cell is thought to preferentially respond to distinct molecular features of odors. Therefore, in the earliest stages of olfaction, sensory information is encoded by combinations of activated ORNs and M/T cells (Rubin and Katz, 1999; Uchida et al., 2000; Wachowiak and Cohen, 2001).

Although odors are deconstructed into their molecular components at early stages of sensory processing, psychophysical studies indicate that odors are perceived as singular percepts rather than a combination of simpler, independent components (Jinks and Laing, 1999; Laing and Francis, 1989). It thus follows that these individual, molecularly defined components must be integrated and combined downstream of the olfactory bulb.

*Correspondence: kf2189@columbia.edu
[2] Present address: Center for Neurobiology & Behavior, Columbia University, New York, New York 10032.

M/T cell axons exit the bulb via the lateral olfactory tract (LOT) and project to the piriform cortex, where they make synaptic contacts with layer II/III pyramidal cells. Recent anatomical studies suggest that the projections of M/T cell axons from individual glomeruli onto cortical pyramidal cells are stereotyped, diffuse, and overlapping (Illig and Haberly, 2003; Zou et al., 2001, 2005). It has been proposed that olfactory cortex pyramidal cells integrate and synthesize the discrete odorant information from different M/T cells, thus enabling single pyramidal cells to represent complex odor information (Buck, 1996; Haberly, 2001; Mori et al., 1999; Wilson and Stevenson, 2003).

How cortical pyramidal cells integrate the odor-driven output of the olfactory bulb will depend upon the relative strength of LOT synapses and the threshold for firing action potentials (APs) in cortical pyramidal cells. If M/T cell inputs onto individual pyramidal cells are weak, activation of individual cortical cells will require many coincident inputs, presumably reflecting a large number of different odorant molecular features. This scheme would allow complex odors to be represented by very few cortical cells. In contrast, cortical cells can be driven with coactivation of only a few inputs if each input is relatively strong, in which case odor representation would entail activation of a large number of cortical cells. Here, we show that single M/T cells can make powerful connections onto cortical pyramidal cells and that coincident activation of only a few M/T cells is sufficient to drive spiking in cortical pyramidal cells.

Results

We made voltage-clamp recordings (V_m = −80 mV) from layer II/III pyramidal cells in rat piriform cortex slices (Franks and Isaacson, 2005). Experiments were typically performed in the presence of the $GABA_A$ antagonist picrotoxin (100 μM) to isolate excitatory responses. We first evoked monosynaptic excitatory postsynaptic currents (EPSCs) by stimulating the LOT through a range of stimulus intensities. We reasoned that more M/T cell axons would be recruited with increasing stimulus strength. As illustrated by the responses shown in Figure 1A, we observed an incremental increase in EPSC amplitude with stronger stimulation (EPSC amplitude evoked by 40–60 V stimulation, 800 ± 180 pA, n = 7 cells), indicating that pyramidal cells receive inputs from many M/T cells.

Myelinated M/T cell axons in the LOT give rise to unmyelinated axon collaterals that branch off at right angles and make synaptic contacts onto pyramidal cells (Ramón y Cajal, 1909; Price and Sprich, 1975). We next used a focal stimulating electrode in the LOT to evoke EPSCs from single M/T cell axons using minimal stimulation (Franks and Isaacson, 2005; Stevens and Wang, 1995). Under these conditions, failures and successes of transmission could be clearly resolved (Figure 1B). While some single fibers were weak (~10 pA, Figure $1B_1$), surprisingly, the amplitudes of many single-fiber EPSCs were very large (>100 pA, Figures $1B_2$ and $1B_3$).

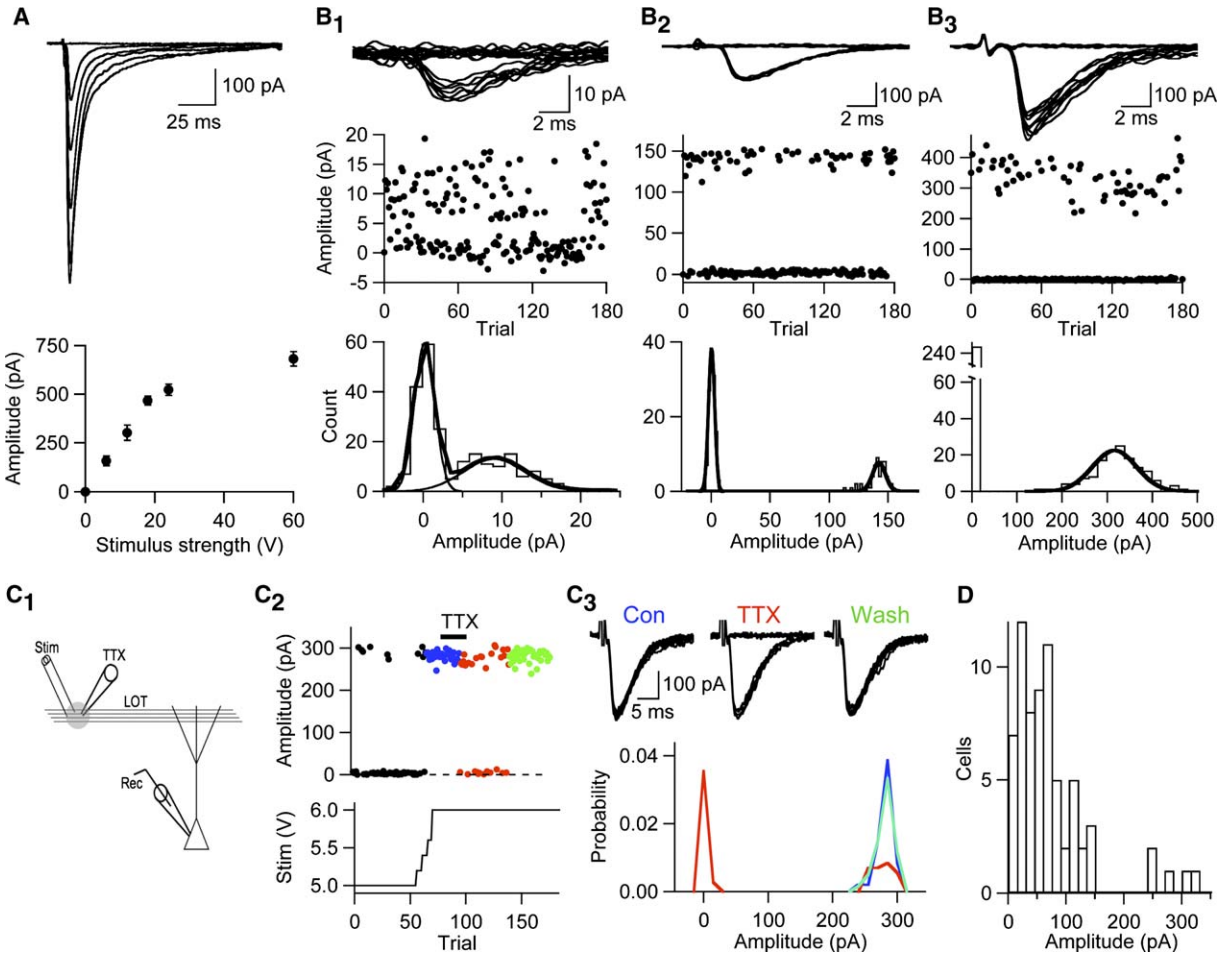

Figure 1. Single M/T Cells Can Make Powerful Connections with Pyramidal Cells

(A) Cortical pyramidal cells receive multiple M/T cell inputs. (Top) Representative experiment showing EPSCs evoked in a cortical pyramidal cell with increasing stimulus strength (average of ten consecutive trials). (Bottom) EPSC amplitude shown as a function of stimulus strength.

(B) Single-fiber inputs in three cells. (Top) Responses from each cell. (Middle) EPSC amplitudes. (Bottom) Amplitude histograms fit with Guassians to successes and failures (B_1 and B_2).

(C) Focal TTX (100 nM) application confirms that minimal stimulation evokes single-fiber responses. (C_1) Recording configuration. (C_2) (Top) EPSC amplitude versus trial number of a minimal stimulation experiment initially showing a large proportion of failures (black). Stimulus strength (bottom) was gradually increased until it was slightly above threshold for reliably evoking responses (blue). TTX was applied by pressure ejection (bar, 50 ms/1 Hz) until failures occurred (red). Reliable responses returned following washout of TTX (green). (C_3) Ten consecutive traces (top) and probability distributions of response amplitudes (bottom) during each of the periods in (C_2).

(D) Single-fiber amplitude summary (successes only, n = 69 cells).

Although our minimal stimulation experiments suggest that single M/T cell axons can make strong connections with pyramidal cells, this approach relies on the assumption that large, all-or-nothing EPSCs result from a single fiber that is being activated near threshold for action potential initiation. However, it might be argued that strong responses instead reflect the simultaneous recruitment of a large number of weaker fibers, each with similar action potential thresholds. To address this concern, we isolated large, all-or-none EPSCs (125 ± 54 pA, n = 5 cells) and used focal puffer application of a low concentration of TTX (100 nM) to slightly raise action potential threshold near the LOT stimulation site (Figure 1C_1). Focal TTX application caused a marked increase in the rate of failures of transmission (control, 16% ± 8%; TTX, 76% ± 6%) that were interspersed with successful responses identical in amplitude (128 ± 54 pA) to those evoked under control conditions (Figures 1C_2 and 1C_3). These results make it highly unlikely that strong all-or-none EPSCs reflect the coactivation of many weak inputs. Rather, the data are most consistent with the notion that minimal stimulation in the LOT can be used to isolate responses elicited from a single M/T cell axon. In total, we recorded single-fiber responses from 69 cells and found a large range of EPSC amplitudes (range, 10–350 pA; median, 59 pA; standard deviation, 68 pA; Figure 1D). These results indicate that single M/T cells can make powerful connections with pyramidal cells.

Do pyramidal cells receive only strong or only weak sensory inputs? To examine this, we used graded stimulation to recruit multiple inputs converging onto pyramidal cells. All-or-nothing steps in EPSC amplitude were used to determine the strength of each recruited M/T cell axon (Figures 2A and 2B). Although some cells had multiple strong inputs (e.g., Figure 2B), the majority

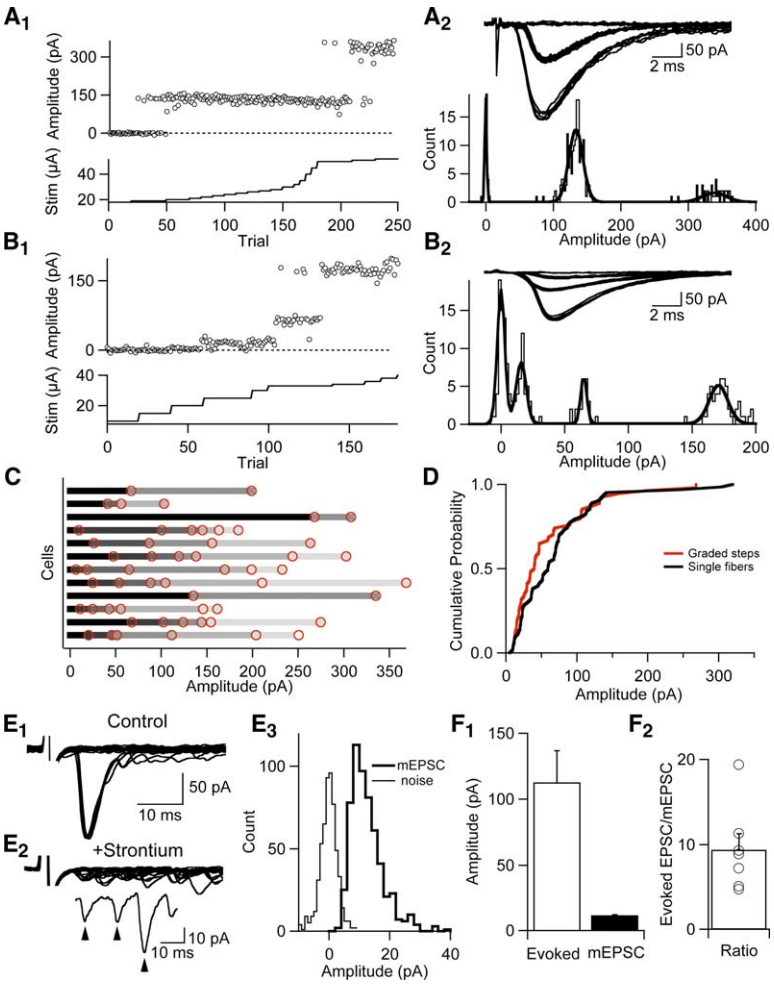

Figure 2. Pyramidal Cells Receive Weak and Strong Connections from Different M/T cells

(A_1) Graded stimulation experiment showing EPSC amplitude (top) and stimulus strength (bottom). (A_2) Traces (top) and amplitude histogram with Gaussian fit.

(B) Results from another pyramidal cell.

(C) Graded steps (circles) in EPSC amplitude for 12 cells.

(D) Distribution of EPSC amplitudes using graded steps and minimal stimulation.

(E) Quantal EPSC amplitude of single fibers. Control responses (E_1) and with Ca^{2+} replaced by Sr^{2+} (E_2). (Inset) Single trial showing three mEPSCs (arrowheads). (E_3) Histogram of mEPSC amplitudes from the same cell.

(F) Quantal content at LOT synapses. (F_1) Summary of evoked EPSC and mEPSC amplitudes. (F_2) Average ratio of evoked versus mEPSC amplitudes. Circles represent ratios for individual cells.

Error bars represent mean ± SEM.

received both weak and strong inputs (Figures 2B and 2C). The amplitudes of graded steps (60 ± 8 pA, n = 55 inputs/12 cells) were in good agreement with our minimal stimulation experiments (Figure 2D, Kolmogorov-Smirnov test, p = 0.1). These results indicate that olfactory sensory inputs with a range of potencies converge onto single pyramidal cells.

To probe the mechanisms underlying large single-fiber EPSCs, we desynchronized transmission to the level of individual quanta (Xu-Friedman and Regehr, 2000). We first measured single-fiber responses, defined by large, all-or-nothing responses evoked in normal extracellular recording solution (Figure 2E_1). We then substituted extracellular Ca^{2+} with Sr^{2+} and measured the amplitudes of the resultant miniature EPSCs (mEPSCs, Figures 2E_2 and 2E_3). To determine a lower bound on the average number of quantal events underlying synaptic transmission at LOT synapses, we divided the mean amplitude of EPSCs evoked under control conditions (113 ± 24 pA, n = 7) by the average size of the mEPSC recorded in each cell (12 ± 0.6 pA, Figure 2F_1). The quantal content (Del Castillo and Katz, 1954), measured in this manner, averaged 9.4 ± 1.9 (Figure 2F_2). These data indicate that strong single-fiber inputs reflect release of multiple quanta. The simplest interpretation is that single M/T cell axons can make multiple synaptic contacts with individual pyramidal cells. Given the median size of all single-fiber evoked responses, ~60 pA, and a quantal size of ~12 pA, our results imply that M/T cell axons make, on average, approximately five functional contacts onto each pyramidal cell.

Olfactory information from the bulb is integrated and transformed by cortical pyramidal cells into output represented by action potential firing (APs). A fundamental feature of this integration is the relationship between presynaptic input and postsynaptic output. We used cell-attached patch recordings to determine this relationship between sensory input strength and AP threshold. LOT stimulation was set such that AP capacitative transients occurred on 50% of trials (Figure 3A). The patch was then ruptured to measure EPSC amplitudes evoked at the same stimulus intensity (Figure 3A). Sensory inputs evoked single APs with a short latency that coincided with the peak of the underlying EPSC (Figures 3A_2 and 3A_3). On average, the EPSC amplitude required to reach AP threshold was 308 ± 45 pA (Figure 3A_3, n = 6 cells). Given the strong potencies of some single fibers, coincident input from only a few M/T cells can be sufficient to drive pyramidal cells to spike.

M/T cells respond to odors in vivo by firing bursts of APs that are time locked to the respiratory cycle (Cang and Isaacson, 2003; Margrie and Schaefer, 2003). To mimic this behavior, we studied the transformation of

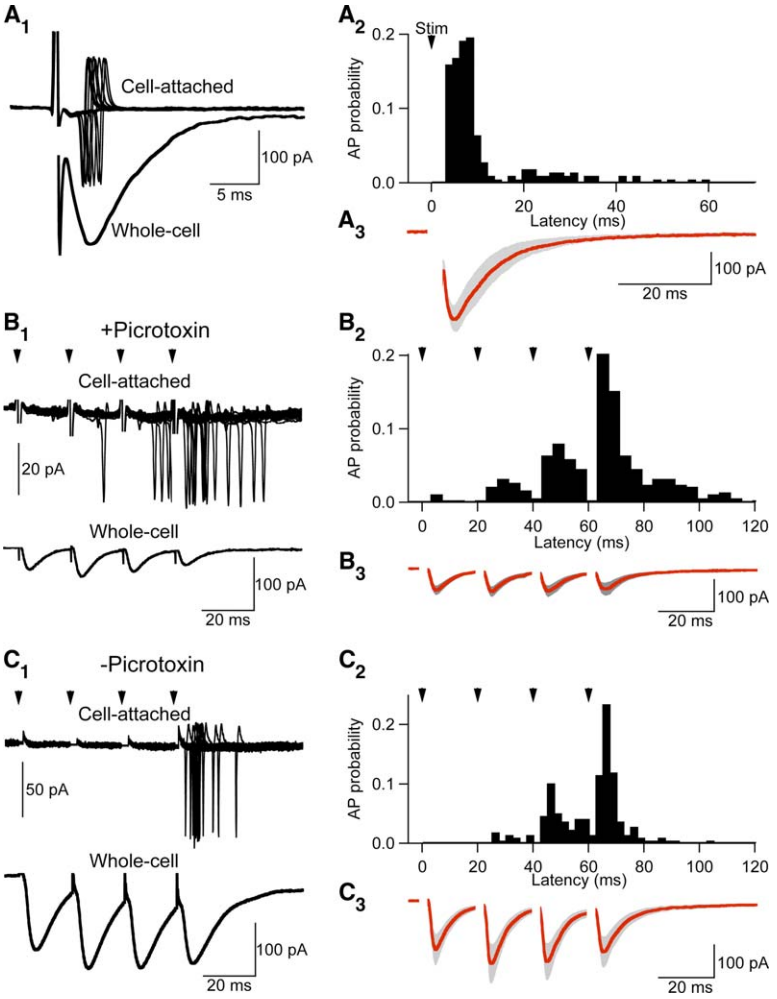

Figure 3. Synaptic Integration in Pyramidal Cells

(A_1) 30 responses to LOT stimulation in cell-attached mode and the average whole-cell EPSC. (A_2) AP latency for spikes in six cells. (A_3) Average (red) and SEM (gray) of the EPSC from all cells.

(B) AP threshold during brief stimulus trains (arrowheads).

(C) As in (B), but without picrotoxin.

synaptic input to AP output during brief stimulus trains (four pulses, 50 Hz, Figure 3B_1). LOT stimulation was again set so that single APs were evoked on 50% of trials. Under these conditions, AP latency was skewed toward EPSCs later in the train (Figures 3B_1 and 3B_2), indicating a role for temporal summation in spike integration. The average amplitude of the first EPSC in the trains driving APs was 73 ± 15 pA (n = 9). LOT synapses onto cortical interneurons may provide a source of feedforward inhibition that contributes to AP integration in piriform cortex (Kanter et al., 1996; Kapur et al., 1997). To address this possibility, we measured AP threshold in response to brief stimulus trains in the absence of picrotoxin. With inhibition intact, stronger LOT input was required to reach AP threshold, and the average amplitude of the first EPSC in the train was 160 ± 49 pA (n = 9, Figure 3C). This indicates that recruitment of GABAergic inhibition, most likely from feedforward interneurons, regulates the integration of LOT input in pyramidal cells. Nonetheless, these data show that during physiologically relevant patterns of activity, very few M/T cells are likely to be sufficient to drive pyramidal cells to spike.

We next measured the integration time window (Pouille and Scanziani, 2001) for coincidence detection of sensory input in piriform cortex. We used two focal stimulating electrodes to activate independent LOT inputs onto the same cell in current clamp. Stimulus strength was set to evoke a single AP on 50% of trials when both pathways were activated simultaneously. One pathway was then activated over a range of time intervals (t = ±50 ms, 2.5 ms increments) relative to the other (Figure 4A), and AP probability was normalized to t = 0 ms (Figure 4B). On average, the normalized AP probability fell below 50% when inputs were activated at intervals >10 ms (Figure 4C, n = 9 cells). This integration time window limits coincidence detection of multiple sensory inputs to intervals on the order of tens of milliseconds.

Discussion

In this study, we show that the axons of single olfactory bulb M/T cells can have a powerful impact on individual pyramidal cells in olfactory cortex. We find that strong single-fiber LOT inputs reflect the synchronous release of multiple quanta. Ultimately, coincident activation of relatively few M/T cells during a brief integration time window is sufficient to generate AP output from cortical pyramidal cells. Together, these results have several implications regarding the strategies used to represent sensory information in olfactory cortex.

Olfactory information in the olfactory bulb is first encoded as a discrete set of glomerular modules reflecting

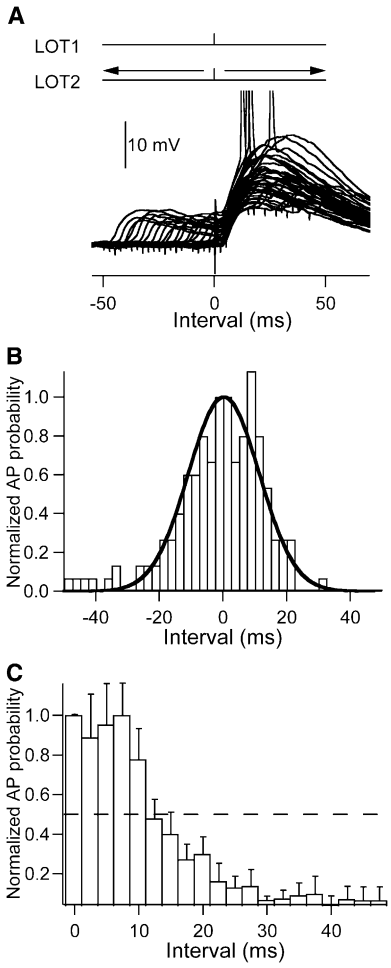

Figure 4. Temporal Integration of Independent LOT Inputs

(A) Integration time window of two LOT inputs in current clamp. Spikes are truncated.

(B) Normalized AP probability versus stimulus interval from the cell in (A).

(C) AP probability versus stimulus interval (positive only) for nine cells. Error bars represent mean ± SEM.

specific molecular features of odorants. How is this information integrated to enable a singular perception of odors (e.g., cinnamon, spearmint)? The olfactory cortex may perform this synthetic process by employing one of two coding strategies.

In one coding approach, each pyramidal cell may receive weak inputs from a large fraction of M/T cells in the bulb. In this case, coincident activation of many different unique types of ORNs, glomeruli, and their ensembles of M/T cells will be required to bring the cortical cell to threshold. A particular odor could then be represented in the cortex by activation of a very small number of pyramidal cells. In this scenario, differences in the overlap and convergence of M/T cell axons onto specific pyramidal cells would generate highly selective neurons that only respond to specific combinations of odorants (e.g., a "cinnamon neuron" versus a "spearmint neuron").

In a different coding strategy, complex odors may be represented in a broad and distributed manner in olfactory cortex if only a few M/T cells are required to activate individual pyramidal cells. According to this model, a combination of odorants with different molecular features would activate multiple cells in olfactory cortex, whose concerted activity will represent the perceived odor. In support of this model, we find that individual M/T cells make strong inputs onto cortical pyramidal cells and that only a few coactive M/T cells are required to bring a pyramidal cell to threshold. This model implies that odor percepts must ultimately derive from the concerted activation of a large population of cortical pyramidal cells. Decoding may require higher brain regions that further process the activity generated from ensembles of active neurons in piriform cortex.

Previous studies have shown that axons in the LOT send branched collaterals into layer Ia of piriform cortex, where they synapse onto pyramidal cell dendrites (Devor, 1976; Ojima et al., 1984; Ramon y Cajal, 1909; Stevens, 1969). We recorded a large range of single-fiber strengths in our experiments and suggest that single LOT axons make multiple synaptic contacts onto single postsynaptic targets—the range of single-fiber strengths reflecting the number of functional synaptic contacts. This heterogeneity of synaptic weights of M/T cell axons onto the same pyramidal cell may also contribute to the need for ensemble olfactory coding in piriform cortex. For example, a given pyramidal cell receives input from many M/T cells. Its activation could therefore represent information reflecting a small subset of odorants (from a few strong M/T cell connections), a complex mixture of odorants (by integrating many coincident weak inputs from different M/T cells), or multiple combinations of strong and weak inputs. Thus, the convergence of sensory inputs with different synaptic weights further limits the significance of information encoded by any one single pyramidal cell.

The response of both M/T and cortical pyramidal cells is time locked to respiration (Cang and Isaacson, 2003; Margrie and Schaefer, 2003; Wilson, 1998) and rats are able to accurately discriminate odors within a single sniff cycle (Abraham et al., 2004; Uchida and Mainen, 2003). Together, these findings require that an upper bound for coincidence detection can be no longer than one respiratory cycle, or the burst duration of M/T cells following inspiration (~100 ms). We show that independent subthreshold LOT inputs sum to threshold efficiently when they occur within ~10 ms. This integration time window in olfactory cortex may be further sharpened by local GABAergic circuits. In support of this idea, we observed that fast inhibition evoked during brief trains of LOT activation raises the threshold for eliciting APs. Overall, integration of coactive M/T cell inputs on a millisecond timescale in pyramidal cells is rapid enough to allow odor discrimination on a sniff-by-sniff basis.

The striking similarity in the anatomical organization of olfactory systems across different phyla may suggest a common, optimal strategy for odor detection and discrimination (Ache and Young, 2005). However, important differences in coding strategies between systems are beginning to emerge. In insects, for example, individual projection neurons in the antennal lobe typically respond to a large number of odorants (Perez-Orive et al., 2002; Stopfer et al., 2003; Wang et al., 2003) and project to Kenyon cells in the mushroom body, which

respond to very few odorants, indicating a "sparsening of the olfactory code" (Perez-Orive et al., 2002). A recent study in mammals, however, reports that individual mitral cells are very narrowly tuned, responding to singular chemical features of an odor (Lin et al., 2005). If each of these M/T cells has diffuse and overlapping projections in the olfactory cortex, and only a few M/T cells are required to drive cortical APs, the olfactory code in the cortex will instead be broadened and distributed.

Experimental Procedures

Experiments followed approved national and institutional guidelines for animal use. Rats (Sprague-Dawley, P12–P32) were anesthetized with pentobarbital (400 mg/kg) and decapitated. The cortices were quickly removed and placed into ice-cold artificial CSF (aCSF) containing (in mM): 83 NaCl, 2.5 KCl, 0.5 $CaCl_2$, 3.3 $MgSO_4$, 1 NaH_2PO_4, 26.2 $NaHCO_3$, 22 glucose, and 72 sucrose, equilibrated with 95% O_2 and 5% CO_2. Parasagittal slices (350 μm) were cut using a vibrating slicer (Vibratome) and incubated at 34°C for 30 min. Slices were then maintained at room temperature until they were transferred to a recording chamber on an upright microscope equipped with differential interference contrast optics (DIC; BX50; Olympus Optical, Tokyo, Japan). All experiments were conducted at 30°C–32°C.

For minimal and graded stimulation recordings, slices were superfused with aCSF containing (in mM): 119 NaCl, 5 KCl, 4 $CaCl_2$, 4 $MgSO_4$, 1 NaH_2PO_4, 26.2 $NaHCO_3$, 22 glucose, and 0.1 picrotoxin, equilibrated with 95% O_2 and 5% CO_2. Baclofen (50 μM) was added to suppress associational synaptic inputs (Franks and Isaacson, 2005). Responses were evoked via a patch pipette (2 μm tip diameter) placed in the LOT. Patch electrodes (3–5 MΩ) contained (in mM): 130 D-Gluconic acid, 130 CsOH, 5 mM NaCl, 10 HEPES, 12 phosphocreatine, 3 MgATP, 0.2 NaGTP, and 10 EGTA. Series resistance, which was always <20 MΩ, was typically compensated at 80%–95%. Synaptic responses were elicited at 0.083–1 Hz. Voltage-clamp and current-clamp responses were recorded with a Multiclamp 700A or Axopatch 200B amplifier (Axon Instruments, Foster City, CA), and responses were filtered at 2 kHz and digitized at 10 kHz. (ITC-18; Instrutech, Mineola, NY). Data were collected and analyzed using Axograph (Axon Instruments) and IGOR Pro (Wavemetrics, Lake Oswego, OR). Summary data are presented as mean ± SEM.

For experiments in which asynchronous release was examined, 4 mM Sr^{2+} was substituted for 4 mM Ca^{2+}. Quantal events were detected and captured within a 200 ms window beginning 200 ms after LOT stimulation using a sliding template algorithm and individually sorted offline. Captured events were discarded if a clear inflection from baseline could not be resolved or if multiple events overlapped during the rising phase of the response.

For recordings of AP threshold and synaptic integration, the aCSF contained (in mM): 119 NaCl, 2.5 KCl, 2.5 $CaCl_2$, 1.3 $MgSO_4$, 1 NaH_2PO_4, 26.2 $NaHCO_3$, 22 glucose, 0.1 picrotoxin, and baclofen was omitted. Patch electrodes contained (in mM): 130 Kmethylsulfate, 5 mM NaCl, 10 HEPES, 12 phosphocreatine, 3 MgATP, 0.2 NaGTP, and 10 EGTA. In cell-attached experiments using a single LOT stimulus to measure AP threshold, spikes were evoked on 52% ± 10% of 90 ± 8 trials (n = 6). For experiments using LOT trains, AP probability was 50% ± 11% over 100 ± 17 trials in the presence of picrotoxin (n = 9 cells) and 65% ± 10% over 52 ± 7 trials in the absence of drug (n = 9).

Acknowledgments

We thank Massimo Scanziani for helpful discussions. This work was supported by NIDCD R01 DC04682, a McKnight Scholar award, and a Klingenstein Fellowship.

Received: October 19, 2005
Revised: November 30, 2005
Accepted: December 27, 2005
Published: February 1, 2006

References

Abraham, N.M., Spors, H., Carleton, A., Margrie, T.W., Kuner, T., and Schaefer, A.T. (2004). Maintaining accuracy at the expense of speed: stimulus similarity defines odor discrimination time in mice. Neuron *44*, 865–876.

Ache, B.W., and Young, J.M. (2005). Olfaction: diverse species, conserved principles. Neuron *48*, 417–430.

Buck, L.B. (1996). Information coding in the vertebrate olfactory system. Annu. Rev. Neurosci. *19*, 517–544.

Cang, J., and Isaacson, J.S. (2003). In vivo whole-cell recording of odor-evoked synaptic transmission in the rat olfactory bulb. J. Neurosci. *23*, 4108–4116.

Del Castillo, J., and Katz, B. (1954). Quantal components of the end-plate potential. J. Physiol. *124*, 560–573.

Devor, M. (1976). Fiber trajectories of olfactory bulb efferents in the hamster. J. Comp. Neurol. *66*, 31–47.

Firestein, S. (2001). How the olfactory system makes sense of scents. Nature *413*, 211–218.

Franks, K.M., and Isaacson, J.S. (2005). Synapse-specific down-regulation of NMDA receptors by early experience: a critical period for plasticity of sensory input to olfactory cortex. Neuron *47*, 101–114.

Haberly, L.B. (2001). Parallel-distributed processing in olfactory cortex: new insights from morphological and physiological analysis of neuronal circuitry. Chem. Senses *26*, 551–576.

Illig, K.R., and Haberly, L.B. (2003). Odor-evoked activity is spatially distributed in piriform cortex. J. Comp. Neurol. *457*, 361–373.

Jinks, A., and Laing, D.G. (1999). A limit in the processing of components in odour mixtures. Perception *28*, 395–404.

Kanter, E.D., Kapur, A., and Haberly, L.B. (1996). A dendritic GABAA-mediated IPSP regulates facilitation of NMDA-mediated responses to burst stimulation of afferent fibers in piriform cortex. J. Neurosci. *16*, 307–312.

Kapur, A., Lytton, W.W., Ketchum, K.L., and Haberly, L.B. (1997). Regulation of the NMDA component of EPSPs by different components of postsynaptic GABAergic inhibition: computer simulation analysis in piriform cortex. J. Neurophysiol. *78*, 2546–2559.

Laing, D.G., and Francis, G.W. (1989). The capacity of humans to identify odors in mixtures. Physiol. Behav. *46*, 809–814.

Lin, D.Y., Zhang, S.Z., Block, E., and Katz, L.C. (2005). Encoding social signals in the mouse main olfactory bulb. Nature *434*, 470–477.

Margrie, T.W., and Schaefer, A.T. (2003). Theta oscillation coupled spike latencies yield computational vigour in a mammalian sensory system. J. Physiol. *546*, 363–374.

Mombaerts, P., Wang, F., Dulac, C., Chao, S.K., Nemes, A., Mendelsohn, M., Edmondson, J., and Axel, R. (1996). Visualizing an olfactory sensory map. Cell *87*, 675–686.

Mori, K., Nagao, H., and Yoshihara, Y. (1999). The olfactory bulb: coding and processing of odor molecule information. Science *286*, 711–715.

Ojima, H., Mori, K., and Kishi, K. (1984). The trajectory of mitral cell axons in the rabbit olfactory cortex revealed by intracellular HRP injection. J. Comp. Neurol. *230*, 77–87.

Perez-Orive, J., Mazor, O., Turner, G.C., Cassenaer, S., Wilson, R.I., and Laurent, G. (2002). Oscillations and sparsening of odor representations in the mushroom body. Science *297*, 359–365.

Pouille, F., and Scanziani, M. (2001). Enforcement of temporal fidelity in pyramidal cells by somatic feed-forward inhibition. Science *293*, 1159–1163.

Price, J.L., and Sprich, W.W. (1975). Observations on the lateral olfactory tract of the rat. J. Comp. Neurol. *162*, 321–336.

Ramón y Cajal, S. (1909). Histologie du systeme nerveux de l'homme et des vertebres (Paris: A. Maloine).

Rubin, B.D., and Katz, L.C. (1999). Optical imaging of odorant representations in the mammalian olfactory bulb. Neuron *23*, 499–511.

Stevens, C.F. (1969). Structure of cat frontal olfactory cortex. J. Neurophysiol. *32*, 184–192.

Stevens, C.F., and Wang, Y. (1995). Facilitation and depression at single central synapses. Neuron *14*, 795–802.

Stopfer, M., Jayaraman, V., and Laurent, G. (2003). Intensity versus identity coding in an olfactory system. Neuron *39*, 991–1004.

Uchida, N., and Mainen, Z.F. (2003). Speed and accuracy of olfactory discrimination in the rat. Nat. Neurosci. *6*, 1224–1229.

Uchida, N., Takahashi, Y.K., Tanifuji, M., and Mori, K. (2000). Odor maps in the mammalian olfactory bulb: domain organization and odorant structural features. Nat. Neurosci. *3*, 1035–1043.

Wachowiak, M., and Cohen, L.B. (2001). Representation of odorants by receptor neuron input to the mouse olfactory bulb. Neuron *32*, 723–735.

Wang, J.W., Wong, A.M., Flores, J., Vosshall, L.B., and Axel, R. (2003). Two-photon calcium imaging reveals an odor-evoked map of activity in the fly brain. Cell *112*, 271–282.

Wilson, D.A. (1998). Habituation of odor responses in the rat anterior piriform cortex. J. Neurophysiol. *79*, 1425–1440.

Wilson, D.A., and Stevenson, R.J. (2003). The fundamental role of memory in olfactory perception. Trends Neurosci. *26*, 243–247.

Xu-Friedman, M.A., and Regehr, W.G. (2000). Probing fundamental aspects of synaptic transmission with strontium. J. Neurosci. *20*, 4414–4422.

Zou, Z., Horowitz, L.F., Montmayeur, J.P., Snapper, S., and Buck, L.B. (2001). Genetic tracing reveals a stereotyped sensory map in the olfactory cortex. Nature *414*, 173–179.

Zou, Z., Li, F., and Buck, L.B. (2005). Odor maps in the olfactory cortex. Proc. Natl. Acad. Sci. USA *102*, 7724–7729.